

Shear Thinning of Noncolloidal Suspensions

Adolfo Vázquez-Quesada,¹ Roger I. Tanner,² and Marco Ellero¹

¹*Zienkiewicz Centre for Computational Engineering, Swansea University, Swansea SA1 8EN, United Kingdom*

²*School of Aerospace, Mechanical and Mechatronic Engineering, University of Sydney, Sydney, New South Wales 2006, Australia*

(Received 21 January 2016; published 31 August 2016)

Shear thinning—a reduction in suspension viscosity with increasing shear rates—is understood to arise in colloidal systems from a decrease in the relative contribution of entropic forces. The shear-thinning phenomenon has also been often reported in experiments with noncolloidal systems at high volume fractions. However its origin is an open theoretical question and the behavior is difficult to reproduce in numerical simulations where shear thickening is typically observed instead. In this letter we propose a non-Newtonian model of interparticle lubrication forces to explain shear thinning in noncolloidal suspensions. We show that hidden shear-thinning effects of the suspending medium, which occur at shear rates orders of magnitude larger than the range investigated experimentally, lead to significant shear thinning of the overall suspension at much smaller shear rates. At high particle volume fractions the local shear rates experienced by the fluid situated in the narrow gaps between particles are much larger than the averaged shear rate of the whole suspension. This allows the suspending medium to probe its high-shear non-Newtonian regime and it means that the matrix fluid rheology must be considered over a wide range of shear rates.

DOI: 10.1103/PhysRevLett.117.108001

Predicting the rheology of particles suspended in simple and complex fluids represents a formidable problem both from a theoretical point of view and also in practical industrial applications [1,2]. Rheological analysis is conventionally done via experiments aimed at the measurement of viscosity and normal stresses under controlled viscometric conditions. A monodispersed suspension of solid spheres in a Newtonian medium represents an ideal case of study. However, despite its apparent simplicity, it is remarkable that even this system is still far from being understood. In the case of colloidal suspensions, where Brownian motion is relevant, accurate predictions of the suspension rheology exist, and shear thinning is observed as result of a decreasing relative contribution of entropic forces at large shear rates [2].

In the noncolloidal limit, however, significant disagreement between simulation, theory, and experiment still exists. Simulations have been very successful in reproducing the shear-thickening behavior, both in its “continuous” and “discontinuous” manifestation. For example, Stokesian dynamics simulations of particles interacting via hydrodynamic lubrication have shown that mild continuous shear thickening can be related to the presence of large fluctuations in the particle density, termed “hydroclusters,” occurring at large shear rates [3–5]. In the thin gaps between particles inside hydroclusters, diverging lubrication forces are active which in turn induce larger stresses in the system, leading to shear thickening [6]. For ideal non-Brownian hard-sphere suspensions thickening might be associated with the presence of surface roughness and also finite particle inertia [7,8] which can all lead to anisotropic microstructure and

shear-rate dependent rheological properties. More recently, also discontinuous shear thickening [9–11] has been successfully reproduced by proposing new granularlike models where additional frictional forces are acting between particles [12–16]. Frictional contact dynamics is expected to dominate especially at large volume fractions, close to jamming transition, and is responsible for the sudden (discontinuous) jump in the viscosity. Recently in [17] the authors showed that frictional contact might represent the relevant contribution even in continuous shear thickening, although as shown in [18] confinement can play an enhancement role too based on pure lubrication dynamics.

A striking rheological phenomenon, however, is observed in noncolloidal suspensions where, well before the onset of shear thickening, shear-thinning behavior has been often reported in experiments [19–22]. In these experiments particles with radii larger than 20 μm were typically used, reaching Péclet numbers in excess of 10^7 for which Brownian effects are practically negligible [21]. Effects due to confinement [19], particle migration, and or sedimentation were ruled out in [19,21]. Despite this phenomenon having been known for a long time [23–25], neither simulation nor theory is capable of predicting it and offering a plausible physical explanation [26,27].

Recently in [28] it was proposed that particle aggregation might take place during steady shear, relating the shear thinning to a decreasing size of these structures at increasing shear rate. Although being a possible mechanism, it does not explain the mismatch between experiments and theory as this hydrodynamic phenomenon has never been predicted in simulations to date.

Another possibility to explain the shear thinning relates to the argument of Wyart and Cates [9], where interparticle friction is included. If the friction diminishes with shear rate then one would expect shear thinning to occur. This possible effect, however, requires the development of new models for frictional contacts being the current ones delivering opposite shear-thickening behavior [13] and, if present, it would be likely to take place at larger volume fractions. Here we will not consider this possibility, and will concentrate on the properties of the matrix.

The non-Newtonian properties of the suspending matrix were considered not relevant in [21]. In that work a Dow Corning silicone fluid was used as suspending medium with negligible shear thinning (less than 10%) in a range of applied input shear rates $\dot{\gamma}_{\text{in}} \in [0.01:100] \text{ s}^{-1}$. In [19,28] the same suspension phenomenology was reported with different suspending fluids, e.g., pure corn syrup, water-glycerin mixture, corn syrup-glycerine mixture, and Shin-Etsu silicone oil. In all cases suspending fluid rheology was reported to be nominally Newtonian within the range of shear rates investigated.

In this Letter, we focus on the “ansatz” of Newtonian property and show that even small *hidden* non-Newtonian effects of the suspending matrix, i.e., those occurring at high shear rates (well above the range probed in the experiments), can produce significant shear thinning of the suspension in the low shear-rate regime under study. Questioning of the Newtonian properties of the suspending media is motivated by the established literature on Dow Corning silicon fluids [29]. Constant Newtonian viscosity is guaranteed by the manufacturer only up to shear rates in the order of 1000 s^{-1} for the polydimethylsiloxane-based (PDMS) fluid at low-molecular weights (e.g., zero shear-rate viscosity $\eta_0 \approx 1 \text{ Pa s}$), as used in [21]. On the other hand, PDMS liquids could shear thin significantly for shear rates above that value [30,31]. Note that the critical shear rate for possible onset of shear-thinning effects is just one order of magnitude larger than the maximum averaged shear rate probed in parallel-plate rheometers used in [21]. At larger shear rates, the fracture of the sample was observed.

Here we modify the suspension model presented in [32] for noncolloidal suspensions. The numerical method used is smoothed particle hydrodynamics (SPH), which is a Lagrangian meshless particle method to describe Navier-Stokes equations. The model can be also extended to incorporate thermal fluctuations and describe Brownian conditions [33]. Whereas long-range hydrodynamic interactions between suspended particles are correctly represented by SPH-mediated forces, short-range pairwise lubrication forces are incorporated directly and solved efficiently by a novel implicit splitting strategy [32,34]. A snapshot of the particle configuration is depicted in Fig. 1. This corresponds to system size $L_x \times L_y \times L_z = (32a, 32a, 32a)$ where a is the radius of the spheres.

The resulting scheme has been used to investigate hydrodynamic shear thickening of hard spheres under confinement in [18] and recently extended to 3D situations [34]. In this Letter, the classical interparticle normal and tangential lubrication forces between two spheres suspended in Newtonian fluid [34] are modified to take into account the specific non-Newtonian behavior of the matrix. For instance, the normal force

$$\mathbf{F}_{\alpha\beta}^{\text{lub}}(s) = -6\pi\eta_0 \left(\frac{a_\alpha a_\beta}{a_\alpha + a_\beta} \right)^2 \frac{1}{s} (\mathbf{V}_{\alpha\beta} \cdot \mathbf{e}_{\alpha\beta}) \mathbf{e}_{\alpha\beta} \quad (1)$$

is modified, by replacing the constant η_0 with a function of the local suspending medium shear rate $\eta(\dot{\gamma})$. In Eq. (1) $\mathbf{e}_{\alpha\beta}$ is the unit vector joining the centers of mass of two suspended solid particles α and β , $\mathbf{V}_{\alpha\beta}$ is their relative velocity, a_α and a_β are their radii, and s is the distance in the gap between sphere-sphere surfaces. In this Letter, we consider $a \equiv a_\alpha = a_\beta = 1$, whereas fluid properties are chosen such that the particle Reynolds number $\text{Re}_p = \rho_0 a^2 \dot{\gamma} / \eta_0 \ll 1$. Moreover, we consider a non-Newtonian model for the suspending fluid which reads

$$\eta(\dot{\gamma}) = \eta_0 \begin{cases} 1, & \dot{\gamma} < \dot{\gamma}_c \\ \left(\frac{\dot{\gamma}}{\dot{\gamma}_c} \right)^m, & \dot{\gamma} \geq \dot{\gamma}_c \end{cases} \quad (2)$$

where η_0 is the constant low shear-rate solvent viscosity, m defines the slope of high shear-rate viscosity decay, and $\dot{\gamma}_c$ denotes the critical shear rate for the onset of shear thinning in the suspending fluid. Effects of changing parameters $\dot{\gamma}_c$ and m will be explored, however, we anticipate that values have been chosen in the range of those encountered for typical suspending media as silicone fluids, with $\dot{\gamma}_c \gg \dot{\gamma}_{\text{in}}^{\text{max}}$, where $\dot{\gamma}_{\text{in}}^{\text{max}}$ is the maximal applied shear rate probed in the viscometric flow between two plates, i.e., $\dot{\gamma}_{\text{in}}^{\text{max}} = 2V_{\text{max}}/H$, where $H = L_z$ (Fig. 1) is the channel gap and V_{max} the maximal plate velocity.

We should point out that this is an approximate approach to take into account the shear-thinning effect in the lubrication interaction. In fact, shear-thinning rheology modifies the parabolic profile for the squeezing flow in and out of the sphere-sphere gap, as assumed in classical lubrication theory [35], and therefore the effective lubrication force cannot be formally cast in the framework of Eq. (1). Unfortunately, there is no exact lubrication expression for the shear-thinning solvent model (2). Nevertheless, we do not expect the general results to be different for a more exact formulation. As the focus here is rather on a proof of concept of the qualitative role of shear thinning we expect the formula adopted in Eqs. (1) and (2) to be sufficiently accurate for our purpose.

As in Refs. [18,34], a shear rate is applied to the sample by moving upper and lower planar solid walls with equal and opposite velocities $\pm V_w$ to reproduce a uniform shear flow. As an effect of the confinement, the input shear rate

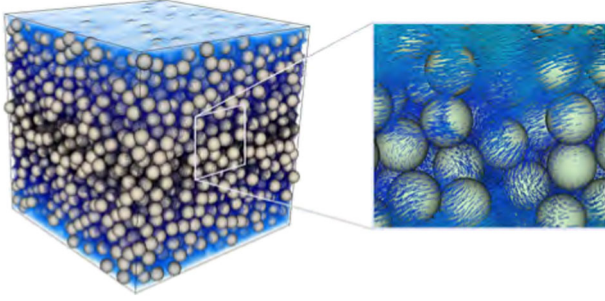


FIG. 1. Snapshot of a simulation corresponding $\phi = 0.4$ and box size $L_z = H = 32a$. Total number of solid particles (gray) was $N_c = 3129$ and SPH fluid particles (blue) $N \approx 4.3 \times 10^6$. For clarity, upper and lower walls have not been drawn. To rule out finite size effects simulations were conducted up to gap size $H = 64a$.

defined as $\dot{\gamma}_{in} = 2V_w/H$ might be slightly different to the real shear rate effectively experienced by the suspension. In order to take into account this effect, similarly to experiments, we correct it by interpolating the linear velocity profile in the bulk region [18], therefore eliminating possible artifacts due to wall slip.

Finally, suspension viscosity is calculated by measuring the force F_x acting on the plates in the flow direction x , via $\eta_{susp} = \sigma_{xz}/\dot{\gamma}_{in} = F_x/L_x L_y \dot{\gamma}_{in}$. Rheology of a Newtonian suspension was investigated in [34] for the relative viscosity $\eta_{rel} = \eta_{susp}/\eta_0$ vs $\dot{\gamma}_{in}$ and η_{rel} vs solid volume fraction $\phi = N4\pi a^3/(3V)$ (N being the total number of suspended spheres) showing results in excellent agreement with previous data [5,36], i.e., constant viscosity plateau under dilute conditions and weak shear thickening in the concentrated regime.

We focus first on the distribution of local shear rates within the fluid domain of a fully Newtonian fluid— η_0 constant—for a typical particle distribution shown in Fig. 1 at $\phi = 0.4$. At this concentration local shear rates cannot be accurately captured by a SPH interpolation of fluid particles, resolution being too coarse in the gap between suspended solid spheres. The dynamics in this regime is lubrication dominated and, as a consequence, local shear rates can be estimated based on the lubrication approximation, i.e., by assuming developed squeezing flow. In particular, for each pair of approaching or departing solid spheres with normal relative velocity $V_{\alpha\beta}$, we estimate $\dot{\gamma}_{loc} = 9\|V_{\alpha\beta}\|/(16s)\sqrt{3a/s}$, where s is the surface-surface separation. Values for $\dot{\gamma}_{loc}$ are estimated for every pair of spheres for over 200 independent configurations obtained once the system has reached steady state. As usual [5,18,34,37], dimensionless shear-rate values are taken as $\dot{\gamma}^* = 6\eta_0 a \dot{\gamma}/F_0$, where F_0 is the constant magnitude of the near hard-sphere interparticle repulsion force $\mathbf{F}_{\alpha\beta}^{rep} = F_0 \tau e^{-\tau s}/(1 - e^{-\tau s}) \mathbf{e}_{\alpha\beta}$ with $\tau^{-1} = 0.001a$ determining its range [5,36].

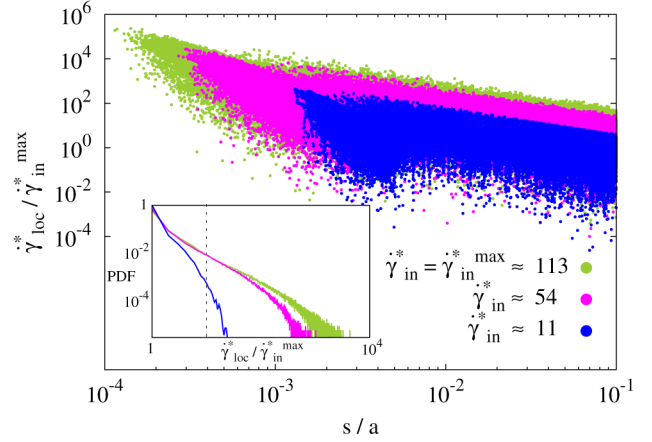


FIG. 2. Simulation of a suspension with Newtonian solvent of constant viscosity η_0 : distribution of the local shear rates $\dot{\gamma}_{loc}^*$ vs gap length between the spheres surfaces and probability distribution of $\dot{\gamma}_{loc}^*$ (inset), for three different input shear rates $\dot{\gamma}_{in}^*$ (vertical dashed line indicates $\dot{\gamma}_c^* = 10\dot{\gamma}_{in}^{*max}$).

Figure 2 shows the distribution of the ratio $\dot{\gamma}_{loc}^*/\dot{\gamma}_{in}^{*max}$ as a function of the dimensionless sphere-sphere separations and for different applied dimensionless shear rates $\dot{\gamma}_{in}^*$. The maximal input shear rate investigated here is $\dot{\gamma}_{in}^{*max} \approx 113$. The distribution of points indicates clearly that at the concentration considered, *locally* in the fluid domain shear rates much larger than the input shear rate are present for particles located at short distances, in agreement with previous scaling arguments [38,39]. For small applied shear rates (blue points), local shear rates are in the order of $\dot{\gamma}_{in}^*$, although rare events with $s < 0.01a$ and $\dot{\gamma}_{loc}^*/\dot{\gamma}_{in}^{*max} \approx 100$ are possible. This distribution stretches towards the left-upper corner for increasing $\dot{\gamma}_{in}^*$ (pink and green points). In these cases distances s smaller than $10^{-3}a$ can occur with resulting $\dot{\gamma}_{loc}^*/\dot{\gamma}_{in}^{*max} > 10^5$.

Note that decreasing interparticle spacing is expected at larger applied shear rates as a result of the accumulation of particles along the compression axis of shear which produces the well-known asymmetric radial distribution function (RDF) [40,41]. The probability distribution function (PDF) of $\dot{\gamma}_{loc}^*$ at equilibrium for three different applied shear rates is depicted in Fig. 2 (inset). Long tails are present for $\dot{\gamma}_{in}^* \approx 54$ and 113 indicating a significant probability for events characterized by very large local shear rates. This observation implies that, if we would consider a critical threshold for shear-thinning rheology in the suspending fluid [Eq. (2)] as $\dot{\gamma}_c^* = 10\dot{\gamma}_{in}^{*max}$ —depicted as a vertical dashed line in the figure—at large shear rates (pink and green lines) there would be a considerable portion of events for which the very high-shear non-Newtonian behavior of the suspending medium would be effectively probed in the interstitial gaps between particles.

As a proof of concept, we have moved from a full Newtonian system to one characterized by Eq. (2), with parameter $m = 0.35$ kept fixed and variable $\dot{\gamma}_c^*$. Figure 3 (top)

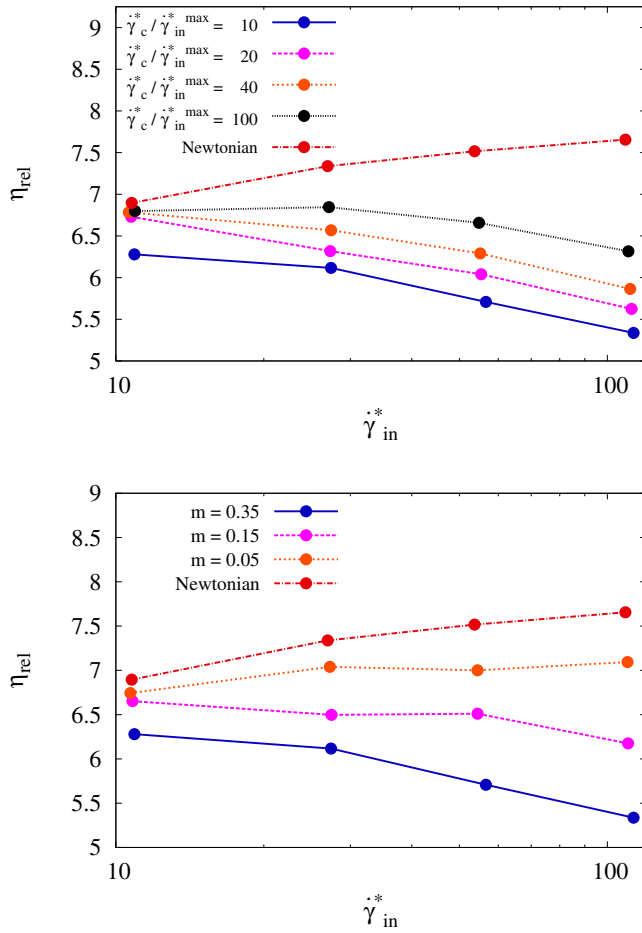


FIG. 3. Rheology of the suspensions with non-Newtonian suspending medium for different $\dot{\gamma}_c^*$ (top) and different slopes of viscosity decay m (bottom).

shows the suspension rheology η_{rel} in the regime $\dot{\gamma}_{\text{in}}^* \in [\dot{\gamma}_{\text{in}}^{*\min}, \dot{\gamma}_{\text{in}}^{*\max}]$. The red line represents the reference Newtonian solution where well-known mild shear thickening is observed as a result of the anisotropic particle RDF. By introducing a *hidden* high-shear power-law behavior η_{rel} , drastic changes occur in the suspension rheology. Even for $\dot{\gamma}_c^*/\dot{\gamma}_{\text{in}}^{*\max} = 100$ the original weak shear-thickening behavior is turned into a slight *shear-thinning* behavior over one order of magnitude in $\dot{\gamma}_{\text{in}}^*$ only. By lowering the ratio $\dot{\gamma}_c^*/\dot{\gamma}_{\text{in}}^{*\max}$ further, i.e., bringing the onset of power-law behavior of the suspending fluid closer to the maximal input shear rate, the shear-thinning behavior of the suspension is visibly enhanced. These results are in remarkable agreement with the phenomenology observed in experiments for noncolloidal systems [19–22,24,25].

In Fig. 3 (bottom) we explore the effect of slope decay m on the resulting shear thinning of the suspension for a fixed ratio $\dot{\gamma}_c^*/\dot{\gamma}_{\text{in}}^{*\max} = 10$. Values of $m \geq 0.1$ seem to change rheological behavior (shear thickening \rightarrow shear thinning) under the described condition. The effect of different thickness ($\tau^{-1} = 0.01a$) on the suspension behavior is

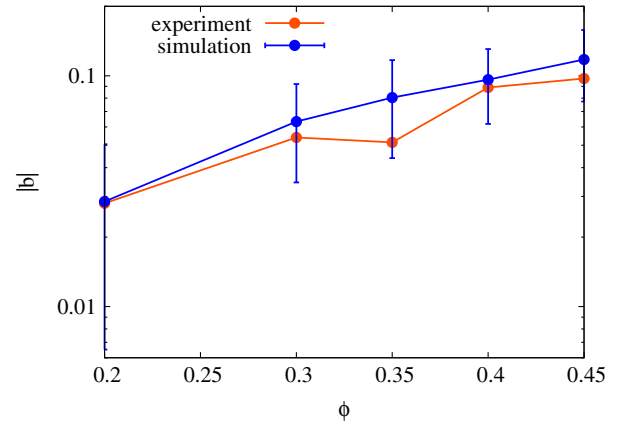


FIG. 4. Power-law exponent b extracted from the suspension viscosity $\eta_{\text{rel}}(\dot{\gamma}_{\text{in}}^*)$ for a solvent fluid characterized by $m = 0.35$ and $\dot{\gamma}_c^*/\dot{\gamma}_{\text{in}}^{*\max} = 10$. Simulations are compared with exponents extracted from experiments in the power-law regime at different concentrations ϕ [21].

presented in the Supplemental Material [42] showing a similar trend. We should stress that typical values matching high-shear behavior of PDMS fluids are in the order of $\dot{\gamma}_c \approx 1000\text{--}5000 \text{ s}^{-1}$ which is 10–50 times larger than the maximal input shear rates investigated in [19,21,25], for example. From [30,31] data, m can be estimated for low-molecular PDMS to be in the range $m \approx 0.01\text{--}0.5$, which is consistent with the values chosen here.

Finally, we explore the effect of solid volume fraction ϕ on the suspension rheology of this system. In practice, we chose parameters $m = 0.35$ and $\dot{\gamma}_c^*/\dot{\gamma}_{\text{in}}^{*\max} = 10$ for the suspending fluid (blue lines in Fig. 3) and vary the total number of suspended spheres N to change $\phi \in [0.2\text{--}0.45]$. All other model parameters are fixed. Figure 4 shows the shear-thinning exponent b of the overall suspension viscosity $\eta_{\text{rel}}(\dot{\gamma}_{\text{in}}^*)$ at different concentrations obtained from algebraical interpolation of the simulated data via $a \times [\dot{\gamma}_{\text{in}}^*]^b$. Results are compared with fitting of the experimental data from [21] in the power-law regime of shear thinning, i.e., for dimensional shear rates $\dot{\gamma}_{\text{in}} \in [0.05\text{--}40] \text{ s}^{-1}$. It is clear that decreasing ϕ has alone the effect of removing the shear thinning, bringing the suspension rheology back to the corresponding Newtonian case at the given concentration. This is characterized by a viscous plateau—exponent b smaller than 0.08—in the semidilute regime ($\phi < 0.35$) in agreement with experiments and previous calculations. This finding can be explained by resorting again to the particle RDF which, under semidilute conditions, does not exhibit strong anisotropic boundary layers in the compressional axis. As a result, particles on average will never get very close to each other, precluding the possibility for having very high local shear rates in the system.

In this Letter we have proposed and tested numerically a possible mechanism for explaining the puzzling shear-thinning behavior often reported in experiments of

noncolloidal suspensions. A non-Newtonian model of interparticle lubrication forces, in combination with the natural highly anisotropic behavior of particle configuration (RDF) present in concentrated systems under shear, allows us to predict experimental observations. The complex microstructural configuration allows us to probe shear-rate regimes of the suspending fluid which would be otherwise hidden when testing its rheology only in a limited (low) range of shear rates. The interplay of this condition with the shear-thinning effects at high shear rates, which are known to appear even in PDMS fluids at low-molecular weight, can finally deliver the observed overall shear thinning of the suspensions. This result suggests also a route to test our assumptions by characterizing the rheological behavior of the suspending media in the very high shear rate regime, e.g., by means of microfluidics-based rheometry [43] or microrheology [44]. This characterization is believed to be particularly relevant for the quantitative prediction of suspension rheology of concentrated systems, still significantly below the maximal critical packing regime where frictional effects should dominate and discontinuous shear thickening is expected [12,13].

M.E. and A.V. gratefully acknowledge the financial support provided by the Welsh Government and Higher Education Funding Council for Wales through the Ser Cymru National Research Network in Advanced Engineering and Materials. Computing resources offered by HPC Wales via the project HPCWT050 are also gratefully acknowledged.

-
- [1] R.I. Tanner, *Engineering Rheology*, 2nd ed. (Oxford University Press, New York, 2000).
- [2] J. Mewis and N. J. Wagner, *Colloidal Suspension Rheology* (Cambridge University Press, Cambridge, 2011), Cambridge Books Online.
- [3] J. F. Brady and G. Bossis, *J. Fluid Mech.* **155**, 105 (1985).
- [4] D. R. Foss and J. F. Brady, *J. Fluid Mech.* **407**, 167 (2000).
- [5] A. Sierou and J. Brady, *J. Rheol.* **46**, 1031 (2002).
- [6] N. J. Wagner and J. F. Brady, *Phys. Today* **62**, 27 (2009).
- [7] P. M. Kulkarni and J. F. Morris, *Phys. Fluids* **20**, 040602 (2008).
- [8] F. Picano, W.-P. Breugem, D. Mitra, and L. Brandt, *Phys. Rev. Lett.* **111**, 098302 (2013).
- [9] M. Wyart and M. E. Cates, *Phys. Rev. Lett.* **112**, 098302 (2014).
- [10] E. Brown, N. A. Forman, C. S. Orellana, H. Zhang, B. W. Maynor, D. E. Betts, J. M. DeSimone, and H. M. Jaeger, *Nat. Mater.* **9**, 220 (2010).
- [11] A. Fall, N. Huang, F. Bertrand, G. Ovarlez, and D. Bonn, *Phys. Rev. Lett.* **100**, 018301 (2008).
- [12] N. Fernandez, R. Mani, D. Rinaldi, D. Kadau, M. Mosquet, H. Lombois-Burger, J. Cayer-Barrioz, H. J. Herrmann, N. D. Spencer, and L. Isa, *Phys. Rev. Lett.* **111**, 108301 (2013).
- [13] R. Seto, R. Mari, J. F. Morris, and M. M. Denn, *Phys. Rev. Lett.* **111**, 218301 (2013).
- [14] R. Mari, R. Seto, J. F. Morris, and M. M. Denn, *J. Rheol.* **58**, 1693 (2014).
- [15] S. Gallier, E. Lemaire, F. Peters, and L. Lobry, *J. Fluid Mech.* **757**, 514 (2014).
- [16] R. Mari, R. Seto, J. F. Morris, and M. M. Denn, *Proc. Natl. Acad. Sci. U.S.A.* **112**, 15326 (2015).
- [17] N. Y. C. Lin, B. M. Guy, M. Hermes, C. Ness, J. Sun, W. C. K. Poon, and I. Cohen, *Phys. Rev. Lett.* **115**, 228304 (2015).
- [18] X. Bian, S. Litvinov, M. Ellero, and N. J. Wagner, *J. Non-Newtonian Fluid Mech.* **213**, 39 (2014).
- [19] I. E. Zarraga, D. A. Hill, and D. T. Leighton Jr, *J. Rheol.* **44**, 185 (2000).
- [20] A. Singh and P. R. Nott, *J. Fluid Mech.* **490**, 293 (2003).
- [21] S.-C. Dai, E. Bertevas, F. Qi, and R. I. Tanner, *J. Rheol.* **57**, 493 (2013).
- [22] Y. Lin, G. W. H. Tan, N. Phan-Thien, and B. C. Khoo, *J. Non-Newtonian Fluid Mech.* **212**, 13 (2014).
- [23] L. Nicodemo, L. Nicolais, and R. Landel, *Chem. Eng. Sci.* **29**, 729 (1974).
- [24] F. Ferrini, D. Ercolani, B. de Cindio, L. Nicodemo, L. Nicolais, and S. Ranaudo, *Rheol. Acta* **18**, 289 (1979).
- [25] F. Gadala-Maria and A. Acrivos, *J. Rheol.* **24**, 799 (1980).
- [26] R. I. Tanner, *J. Non-Newtonian Fluid Mech.* **222**, 18 (2015).
- [27] C. D. Cwalina and N. J. Wagner, *J. Rheol.* **58**, 949 (2014).
- [28] Y. Lin, N. Phan-Thien, and B. C. Khoo, *J. Non-Newtonian Fluid Mech.* **223**, 228 (2015).
- [29] <http://www.dowcoming.com/content/discover/discoverchem/si-rheology.aspx>.
- [30] T. Kataoka and S. Ueda, *J. Polym. Sci. A* **3**, 2947 (1965).
- [31] C. L. Lee, K. E. Polmanteer, and E. G. King, *J. Polym. Sci. A* **8**, 1909 (1970).
- [32] X. Bian and M. Ellero, *Comput. Phys. Commun.* **185**, 53 (2014).
- [33] X. Bian, S. Litvinov, R. Qian, M. Ellero, and N. A. Adams, *Phys. Fluids* **24**, 012002 (2012).
- [34] A. Vázquez-Quesada and M. Ellero, *J. Non-Newtonian Fluid Mech.* **233**, 37 (2016).
- [35] S. Kim and S. J. Karrila, *Microhydrodynamics: Principles and selected applications* (Dover Publication, 1991).
- [36] E. Bertevas, X. Fan, and R. I. Tanner, *Rheol. Acta* **49**, 53 (2010).
- [37] A. Vázquez-Quesada, X. Bian, and M. Ellero, *Comput. Particle Mech.* **3**, 167 (2016).
- [38] S. Dagois-Bohy, S. Hormozi, É. Guazzelli, and O. Pouliquen, *J. Fluid Mech.* **776** (2015).
- [39] X. Chateau, G. Ovarlez, and K. L. Trung, *J. Rheol.* **52**, 489 (2008).
- [40] A. K. Gurnon and N. J. Wagner, *J. Fluid Mech.* **769**, 242 (2015).
- [41] F. Blanc, E. Lemaire, A. Meunier, and F. Peters, *J. Rheol.* **57**, 273 (2013).
- [42] See Supplemental Material at <http://link.aps.org/supplemental/10.1103/PhysRevLett.117.108001> for results with $\tau^{-1} = 0.01a$.
- [43] C. J. Pipe and G. H. McKinley, *Mech. Res. Commun.* **36**, 110 (2009).
- [44] T. G. Mason and D. A. Weitz, *Phys. Rev. Lett.* **74**, 1250 (1995).